NANO LETTERS

Letter

pubs.acs.org/NanoLett

Electrically Tunable Coherent Optical Absorption in Graphene with Ion Gel

Vrinda Thareja,[†] Ju-Hyung Kang,[†,§] Hongtao Yuan,[§,†] Kaveh M. Milaninia,[†] Harold Y. Hwang,[†,§] Yi Cui,[†,§] Pieter G. Kik,[†,‡] and Mark L. Brongersma*[,†]

[†]Geballe Laboratory for Advanced Materials, Stanford University, Stanford, California 94305, United States

[§]Stanford Institute for Materials and Energy Sciences, SLAC National Accelerator Laboratory, Menlo Park, California 94025, United States

[‡]CREOL, The College of Optics and Photonics, University of Central Florida, 4000 Central Florida Blvd, Orlando, Florida 32816, United States

ABSTRACT: We demonstrate electrical control over coherent optical absorption in a graphene-based Salisbury screen consisting of a single layer of graphene placed in close proximity to a gold back reflector. The screen was designed to enhance light absorption at a target wavelength of 3.2 μm by using a 600 nm-thick, nonabsorbing silica spacer layer. An ionic gel layer placed on top of the screen was used to electrically gate the charge density in the graphene layer. Spectroscopic reflectance measurements were performed in situ as a function of gate bias. The changes in the reflectance spectra were analyzed using a Fresnel based transfer matrix model in which graphene was treated as an infinitesimally thin sheet with a conductivity given by the Kubo formula. The analysis reveals that a careful choice of the ionic gel layer thickness can lead to optical absorption enhancements of up to 5.5 times for the Salisbury screen compared to a suspended sheet of graphene. In addition to these absorption enhancements, we demonstrate very large electrically induced changes in the optical absorption of graphene of ~3.3% per volt, the highest attained so far in a device that features an atomically thick active layer. This is attributable in part to the more effective gating achieved with the ion gel over the conventional dielectric back gates and partially by achieving a desirable coherent absorption effect linked to the presence of the thin ion gel that boosts the absorption by 40%.

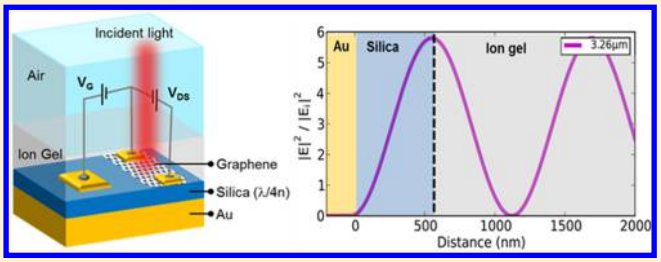

KEYWORDS: *Coherent absorption control, graphene, Salisbury screen, differential reflectance, transfer matrix, ionic gel*

Graphene, a two-dimensional (2D) sheet of hexagonally arranged carbon atoms, has gained significant attention for its unique electrical, optical, and mechanical properties.[1−4] These include its ability to absorb 2.3% of the incident light over a broad range of wavelengths, an extremely high charge carrier mobility on the order of ~200,000 $cm^2/(V{\cdot}s)$ for suspended, high-quality graphene and an extraordinary intrinsic mechanical strength.[5,6] This makes graphene a promising candidate for many applications such as ultrafast photodetectors, modulators, solar cells, and transparent electrodes.[7−11] Whereas the single-layer-absorption is impressive, it is not strong enough for many optoelectronic applications as virtually all the light is transmitted. Moreover, for active devices such as electro-optical modulators and actively controlled thermal emitters, dynamic control over absorption is required as well.[12] In this work, we explore an electrically tunable Salisbury screen device capable of achieving both increased absorption and active absorption modulation in a single graphene sheet.

Recently, there have been a number of excellent efforts directed at enhancing the optical absorption in graphene. For example, plasmonic nanostructures have been used to locally concentrate fields in this 2D material with the aim to increase the efficiency of graphene-based photodetectors.[13,14] Theoretically, complete light absorption in graphene has also been predicted under critical-coupling conditions by cleverly patterning it to tune its conductivity.[15] Integrating graphene with an optical waveguide has been employed to achieve a longer light-graphene interaction length.[16] Graphene microcavity photodetectors have also been demonstrated that produce increased absorption in graphene due to enhanced optical fields inside a high quality factor (Q) resonant cavity.[17]

Here, we demonstrate how the absorption of infrared light in a graphene layer can be boosted by placing it into a Salisbury-screen-type configuration that provides for strong coherent absorption. Furthermore, we show that we can actively tune the absorption in the graphene layer by electrical gating with an ionic gel. Recently, a Salisbury screen optimized for the terahertz (THz) range was demonstrated wherein the absorption in graphene was tuned by chemical doping.[18] An electrically tunable Salisbury screen employing the idea of

Received: October 21, 2014
Revised: February 3, 2015
Published: February 11, 2015

DOI: 10.1021/nl503431d
Nano Lett. 2015, 15, 1570−1576

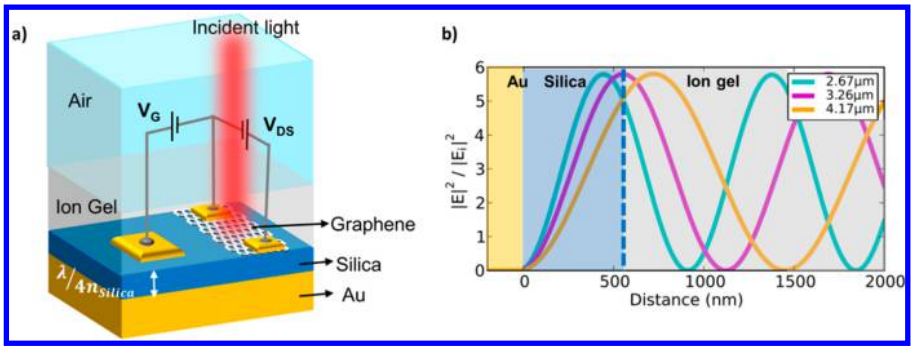

Figure 1. (a) Schematic of the graphene-based Salisbury absorber consisting of a stack with air/ion gel/silica/gold. (b) Square of the electric field (E) magnitude normalized to the square of the incident electric field (E_i) magnitude within the device structure for illumination wavelengths of 2.7, 3.2, and 4.2 μm. The color convention for the different device layers matches those in panel (a). The vertical dotted line at the interface of silica and ion gel represents the position of graphene.

patterning the graphene layer into nanoscale resonators based on the theoretical work previously discussed for achieving complete light absorption in graphene[15] has also been published very recently.[19] Our work is based on an electrical gating scheme with an ionic gel top gate that offers low-voltage (a few volt) operation. Previously, higher operation voltages of 10−100 V were required for devices in which a 1 μm thick Si_3N_4 layer was used as both the optical spacer layer and the back gate dielectric of the screen.[19] This configuration does not allow for lower voltage operation as the optical spacer needs to be thick. Using our gating method, we achieved a record-high modulation of absorption in graphene per unit applied voltage of 3.3% per volt. This is the highest modulation attained so far in a device that features an atomically thick active layer. It is in part due to the more effective electrical gating with the gel and in part because the presence of the thin ionic gel induces an unexpected and a desirable coherent absorption effect that boosts the absorption in the graphene by another 40% over a basic Salisbury screen, as explained later in the paper.

The original Salisbury[20] screen was invented by the American engineer Winfield Salisbury in 1952 and was employed in some of the first radar absorbent materials.[21] In its original implementation, an absorbing layer of graphite (i.e., multilayered graphene) was spaced from a metallic back reflector by a transparent spacer layer. It was shown that (for some target wavelength) the net reflection from the system can be made to vanish and unity absorption can be achieved. To first order, this occurs when the direct reflection from the absorbing layer and the light returning from the back reflector are equal in magnitude and opposite in sign. For this to happen, the spacer layer thickness (t) has to be approximately equal to a quarter of the wavelength of the incident light in the spacer layer with refractive index n_{Spacer}, that is, $t \approx \lambda/4n_{Spacer}$. In a second-order theory, multiple reflections between the screen and the reflector have to be accounted for.

When the mirror is a perfect electrical conductor (PEC) featuring a very high electrical conductivity, the spacer thickness should exactly equal one-quarter of the targeted operation wavelength to maximize absorption. However, real metals at optical frequencies allow for some field penetration (up to a skin depth) and this gives rise to a reflection phase pick up that deviates from that of a perfect electrical conductor. As a result, a thinner spacer layer thickness can be used to achieve the destructive interference condition. The field penetration comes at the cost of some optical losses in the metal. However, when a very strongly absorbing film like graphene is used in conjunction with a real but highly conductive metal reflector it is possible that most of the absorption takes place within the film as opposed to the metal. As a result, an active tuning of the absorption properties of the film can have a significant impact on the reflected signal. In this work, we combine experiment and theory to analyze the nature and magnitude of the absorption changes one can achieve with a graphene-based Salisbury screen device. The operation wavelength will be in the mid-IR spectral range around 3 μm, which is of great importance for many applications that include IR vibrational spectroscopy, sensing, and thermal radiation control.

Figure 1a shows a schematic of our proposed device configuration. It consists of a graphene sheet that is judiciously spaced from a metallic back reflector by a transparent 600 nm thick silicon dioxide (SiO_2) spacer layer. A 200 nm thick gold (Au) film was used as the metal back reflector due to its high reflectance in the mid-infrared (IR) part of the electromagnetic spectrum. The entire stack was deposited on a silicon (Si) substrate by standard electron beam (e-beam) evaporation. The SiO_2 layer was produced by high-density plasma-enhanced chemical vapor deposition (HDPECVD). Commercially available CVD graphene (from ACS Material) was then transferred onto the SiO_2 spacer. Using e-beam evaporation, large gold pads on the order of ~1 cm × 0.5 cm were deposited to serve as source and drain contacts for electrical transport measurements on graphene. A larger, laterally placed Au pad of approximately 2 cm × 1 cm was also deposited to electrically gate and control the carrier density of the graphene sheet with ionic gel. This was followed by spin-coating a smooth, 4.5 μm thick layer of ionic gel, derived from the ionic liquid DEME-TFSI [*N*,*N*-diethyl-*N*-methyl-*N*-(2-methoxyethyl) ammonium bis(trifluoromethylsulfonyl) imide]. The ion gel has a high refractive index that is comparable to that of SiO_2 (n_{gel} = 1.43) and they together form a very low Q optical cavity.[22] The thickness of the spacer layer was chosen such that an incident wave at a target wavelength of ~3.2 μm produces a standing wave with an antinode in the electric field intensity lying at the location of the graphene sheet (Figure 1b). As the electric field magnitude $|E|$ is approximately doubled due to interference effects (except for losses in the graphene and metal) over the incident field magnitude $|E_i|$, the absorption enhancement in graphene, which is linked to $|E|^2/|E_i|^2$, is approximately quadrupled. This choice not only facilitates strong light absorption, it also affords a relative insensitivity of the absorption to the exact position of the screen. In the optical analysis provided later in this manuscript, we also demonstrate

DOI: 10.1021/nl503431d
Nano Lett. 2015, 15, 1570−1576

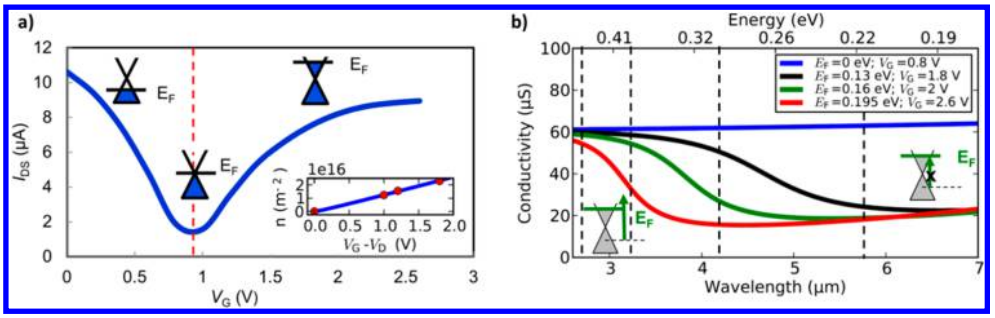

Figure 2. (a) Experimentally determined dependence of the drain-source current (I_{DS}) on gate voltage (V_G). (Inset) Calculated charge carrier density with effective applied gate bias. (b) Calculated spectral dependence of the conductivity of graphene in the mid-infrared spectral range for different Fermi energy level positions/magnitude of the gate bias. The band diagram schematics illustrate the conductivity trends. The conductivity is low at long wavelengths and high at short wavelengths. A high/low value of the conductivity is reached when optical transitions can/cannot be made from the valence to the conduction band. Because of state filling of the conduction band, a minimum amount of photon energy $E_{ph} \approx 2\ E_F$ is required to stimulate an interband transition in graphene.

the significant optical benefits of the ion gel layer in addition to its electrical role of gating the device.

The variation of the drain-source current through the graphene channel with the applied gate bias across the ionic gel is shown in Figure 2a. The measurements were performed using a semiconductor parameter analyzer (Agilent B1500). A constant drain-source voltage (V_{DS}) of 10 mV was applied while monitoring the resultant drain-source current (I_{DS}) as a function of the applied gate bias (V_G). Upon application of a gate bias, ionic charges accumulate at the ionic gel/graphene and ionic gel/gold pad interfaces.[23] This in turn causes the carrier density and hence the conductivity of graphene to change. A minimum in I_{DS} occurs at a gate bias referred to as the Dirac voltage (V_D). This condition corresponds to the charge neutrality point (CNP) in graphene.[24] At the CNP, the Fermi level of graphene passes through the point of intersection of the conduction and valence band. The occurrence of the CNP at a positive V_G (= 0.8 V) indicates that the graphene sheet in our devices was effectively p-doped with the Fermi level lying in the valence band as shown schematically in the band diagram in Figure 2a. The magnitude of I_{DS} increases again for voltages above the CNP due to accumulation of electrons in the conduction band, making graphene effectively n-type.

The electrical data in Figure 2a will be used to predict the bias-dependent reflection properties of the Salisbury screen. To this end, we first describe an equivalent circuit model for our device that links the carrier density/position of the Fermi level to the applied gate voltage. The conductivity σ across the spectral range of interest can in turn be calculated based on the position of the Fermi level using the theoretical formalism developed by Kubo (discussed later). The optical absorption in the structure is proportional to the conductivity and the square of the electric field magnitude at the location of the graphene sheet. An optical (transfer matrix) model is finally constructed to calculate the field distribution and the optical reflection properties for the screen.

The electric double layers (EDLs) formed at the ion gel/graphene and ion gel/gold (Au) pad interfaces serve as capacitor structures with an approximate spacing between the "plates" of a few nanometers.[25] Physically, this effective distance is linked to the spacing of the ions in the gel and the mobile carriers in graphene or Au. We define a total double layer capacitance (C_{EDL}) as the geometric capacitance per unit area of the EDLs formed by the series combination of the Au/ion gel interfacial capacitance and graphene/ion gel interfacial capacitance. At first, one might think that these are the only capacitors at play in the system. However, due to the finite density of states of 2D conductors like graphene, such materials do not behave like the metallic plates of a conventional capacitor structure. Here, one needs to account for the substantial impact of band-filling/band-emptying upon charging/discharging of the 2D graphene "plate" that features a small density-of-states compared to regular metals. To construct useful circuit models for such unusual capacitor plate materials, Luryi introduced the concept of a quantum capacitance (C_Q).[26] He found that one can take into account the band-filling/band-emptying with a second "quantum" capacitance placed in series to the usual geometric capacitance of a parallel plate capacitor.[27] As a result, the applied gate voltage creates both an electrostatic potential difference ϕ across the geometric capacitance and produces a shift in the Fermi level E_F that is linked to the quantum capacitance of graphene[28]

$$|V_G - V_D| = \phi + \frac{E_F}{e} \tag{1}$$

In this equation, e is the electron charge. The magnitude of electrostatic potential $\phi = ne/C_{EDL}$ has a linear dependence on the charge density n similar to that for a regular metal-plate capacitor. On the other hand, the magnitude of E_F is proportional to the square root of the charge density n[29]

$$E_F = \hbar v_F \sqrt{\pi n} \tag{2}$$

Here, v_F is the Fermi velocity and $\hbar$ is the reduced Planck's constant. Taking $C_{EDL} = 1.45 \times 10^{-3}$ F/m^2 as an example, which is a reasonable estimate based on the dielectric properties of the ion gel and the thickness of the double layer (few nanometers), we can plot the estimated charge density n versus effective gate bias $V_G - V_D$ (inset of Figure 2a). It should be noted that these types of estimates of the double layer capacitance tend to be first-order estimates based on the not so well-defined nature of this capacitor structure. With knowledge of the carrier density and eq 1, one can calculate the dependence of E_F on the gate voltage.

The changes in σ that result from bias-induced movements in the Fermi energy level of graphene can be calculated using the Kubo formula[30,31]

DOI: 10.1021/nl503431d
Nano Lett. 2015, 15, 1570−1576

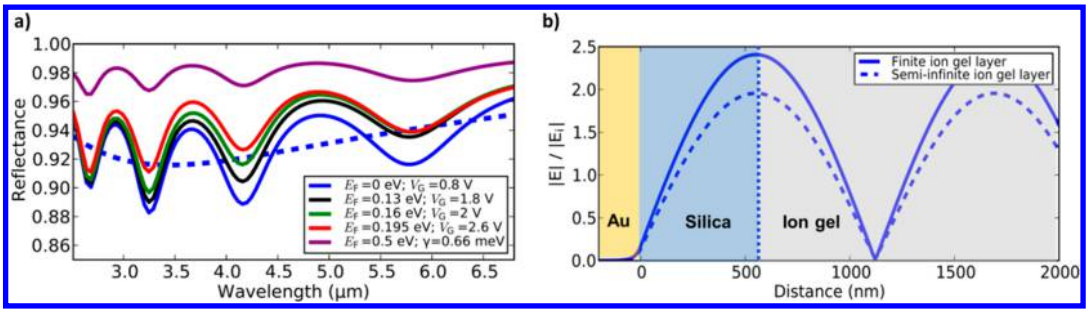

Figure 3. (a) Simulated reflection spectra for the Salisbury screen at different positions of the Fermi energy level in graphene. The dotted blue curve represents the reflectance for a structure with semi-infinite ion gel instead. (b) Absolute value of electric field in the device with a finite thickness ionic gel layer (solid curve) and with a semi-infinite ion gel layer (dotted curve) normalized to the absolute value of the incident electric field (E_i). The vertical dotted line at the interface of silica and ion gel represents the position of graphene.

$$\sigma = -\frac{ie^2}{4\pi\hbar}\ln\frac{2E_F - (\hbar\omega - 2i\hbar\Gamma)}{2E_F + (\hbar\omega - 2i\hbar\Gamma)} - \frac{ie^2 k_B T}{\pi\hbar(\hbar\omega - 2i\hbar\Gamma)}\left[\frac{E_F}{k_B T} + 2\ln(e^{-E_F/k_B T} + 1)\right] \quad (3)$$

where ω is the angular frequency, Γ is the scattering rate for the mobile carriers, k_B is the Boltzmann constant, and T is the temperature. The dependence of conductivity of a graphene sheet on wavelength is plotted in Figure 2b for four different possible locations of the Fermi level: 0 (CNP point), 0.13, 0.16, and 0.195 eV. These values of E_F are achieved at 0.8 (CNP point), 1.8, 2, and 2.6 V respectively. The spectral dependence of σ can be understood by realizing that its magnitude is governed by two major contributions that dominate in different wavelength regimes. At longer wavelengths, the dominant contribution to the conductivity comes from the free-carrier response (i.e., intraband excitations). This contribution is described fairly well by the Drude model. At shorter wavelengths, the optical response is dominated by interband transitions and is independent of wavelength.[32] As a result, the conductivity approaches the well-known universal value of 60 μS at the shorter wavelengths.[33] It can be seen that an increase in the bias voltages causes the conductivity to decrease over the entire wavelength range of interest. The exact functional dependence of conductivity on the applied bias is however different at each wavelength as each of the conductivity curves shows a "swing" from a high to a low value at a photon energy $E_{ph} \approx 2E_F$. This swing is caused by the fact that a minimum amount of photon energy $E_{ph} \approx 2E_F$ is required to stimulate an interband transition in graphene (as dictated by the state filling that is schematically depicted in the two band diagrams in Figure 2b).

In order to theoretically predict the optical response of our graphene-based Salisbury screen in the infrared, a transfer matrix model[34] was used, wherein graphene was treated as an infinitesimally thin sheet with a conductivity given by eq 3. The calculated spectral reflectance curves for this structure at the different Fermi level positions/values of the gate bias are shown in Figure 3a. Each of the reflectance curves shows a series of four Fabry–Perot-like oscillations with pronounced reflection minimums around 2.7, 3.2, 4.2, and 5.8 μm. The magnitude of the free spectral range between the oscillations indicates that the structure serves as an asymmetric Fabry–Perot resonator, where the resonator thickness is equal to the sum of the SiO_2 and ion gel layers. To confirm this point, we compare the calculated reflectance from the Salisbury screen with a finite and semi-infinite ion gel layer for the case of E_F = 0 eV (solid and dashed blue curves in Figure 3a). Because of the absence of the ion gel/air interface for the semi-infinite layer case, there are no oscillations in the reflection curve. Instead, a single reflection minimum is observed at a wavelength of ~3.2 μm. At this wavelength, the electric field shows a maximum value at the location of the graphene sheet (see Figure 1b). The finite thickness of the ionic gel introduces oscillations in the reflectance curve exceeding 4%, corresponding to relative changes in the absorption of a few tens of percent. The fact that the addition of a weakly reflecting interface can cause such large changes in absorption seems surprising at first but can be understood by considering the magnitude of the total electric field at the graphene sheet location. For a free-standing film, the absorption is proportional to the square of the incident electric field, that is, $A_{fr} \propto (E_i)^2$. In the Salisbury screen configuration, the metallic back reflector causes the absolute value of total electric field to periodically vary with distance along the direction of incidence (see Figure 3b). At the location of graphene, the total field is approximately doubled due to constructive interference and the absorption is given by $A_{SB} \propto (2E_i)^2 = 4(E_i)^2$. As such the absorption is increased by a factor 4 over the suspended sheet, that is, $A_{SB}/A_{fr} \approx 4$. The presence of a finite thickness ionic gel introduces one more reflective boundary capable of the redirecting the light that bounced off the Au mirror back into the cavity. The Fresnel amplitude reflection coefficient r for light normally incident from one medium with refractive index n_1 to a material with refractive index n_2 is given by $r = (n_1 - n_2)/(n_1 + n_2)$. This implies that of the field initially reflected by the back Au mirror, ~17% is reflected back into the cavity from the ion gel/air boundary. Depending on the cavity thickness and the wavelength of the light, this additional amplitude can add constructively or destructively at the location of the graphene sheet. It is worth pointing out that the absorption losses in Au are small (<2% over the wavelength range of interest) and virtually bias independent (~0.06% change in absorption over bias variations from 0.8 to 2.6 V). Apart from the small absorption losses in graphene and the Au mirror that incur in the first pass of light through the cavity, the reflected field amplitude can be estimated as $E_r \approx 0.17\ E_i$. As a result, the maximum and minimum absorption that can be attained are given by $A_{max} \propto (2E_i + 2E_r)^2 \approx 5.5E_i^2$ and $A_{min} \propto (2E_i - 2E_r)^2 \approx 2.7E_i^2$. This corresponds to an enhancement or suppression in the absorption of 38% and 33%, respectively, as compared to the semi-infinite ionic gel case. The total enhancement in absorption of the suspended graphene sheet can be as high

DOI: 10.1021/nl503431d
Nano Lett. 2015, 15, 1570–1576

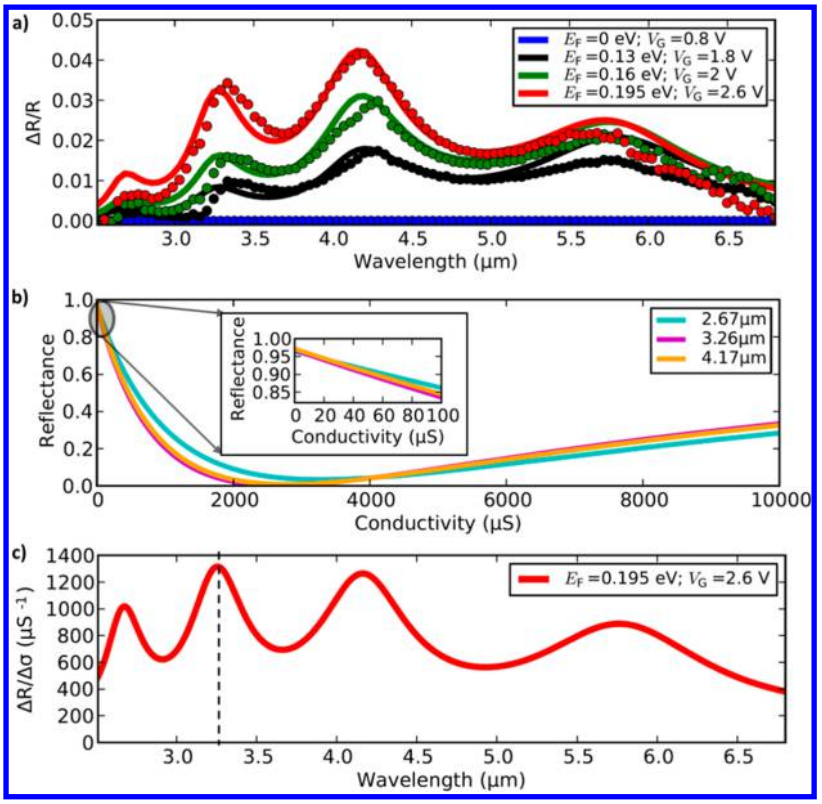

Figure 4. (a) Normalized differential reflectance spectra for different Fermi energy levels in graphene. The dotted lines are the experimental measured values and the solid lines are transfer-matrix model-based vales. (b) Reflectance from an absorbing layer of variable conductivity. (Inset) Zoomed in reflectance for conductivity values in the range of 0−100 μS. (c) Differential change in the optical reflectance from the Salisbury screen with the conductivity of graphene as a function of wavelength.

as 5.5 times for a properly chosen ion gel thickness. It is worth noting that these substantial enhancements are not attributable to a significant buildup of optical energy in the cavity, but rather to a favorable constructive interference of the incident and reflected fields that can be achieved in this particular Salisbury screen configuration. It is also worth pointing out that the subsequent application of an electrical bias primarily changes the depth of the reflection peaks and does not significantly affect the spectral position. Similar to the trend for graphene's conductivity (Figure 2b), a gradual increase in the Fermi level first impacts the spectral reflectance at long wavelengths and then at shorter ones. Using experimentally observable values of mobile carrier scattering rate, $\Gamma \approx 1$ THz, (i.e., $\hbar\Gamma \approx 0.66$ meV) for high quality graphene combined with higher (but realistic) magnitudes of the Fermi level, E_F = 0.5 eV in graphene, it is possible to achieve an absorption modulation of as high as 10% for our design.[35] This is shown as part of Figure 3a. Further enhancements in the absorption modulation can be achieved when graphene is patterned into nanoscale plasmonic resonators.[15,19]

Next, we measured the dependence of the optical response of the fabricated graphene-based Salisbury absorber on gate bias. A Fourier transform infrared (FTIR) spectrometer was employed to measure the reflectance spectra. For practical applications, we are particularly interested in quantifying the ability to modulate the reflectance. To this end, we analyze the normalized differential reflectance $(R_{E_F} - R_D)/R_D$, which is proportional to the difference between the reflectance at a given Fermi energy level of interest (or applied gate bias) R_{E_F} and the reflectance at the CNP given by R_D. On the basis of $I_{DS} - V_G$ measurements (Figure 2a), the CNP for our devices was achieved at an applied bias of 0.8 V. The dots in Figure 4a show measurements of the normalized differential reflectance at gate biases of 0.8, 1.8, 2, and 2.6 V. The solid lines in Figure 4a represent the calculated differential reflectance spectra based on the transfer matrix model at the corresponding Fermi energy levels in graphene of 0, (CNP), 0.13, 0.16, and 0.195 eV (using $C_{EDL} = 1.45 \times 10^{-3}$ F/m^2 as previously mentioned). Good agreement is obtained between experimental and theoretical spectra. The curve corresponding to 0.8 V (E_F = 0 eV) coincides with the horizontal axis since the reflectance at this gate voltage is used as the reference for normalization. The four peaks in this figure occur at the exact spectral locations where the calculated reflectance spectra show peaks (Figure 3a).

Figure 4a shows that the largest change in reflectance due to a Fermi level change from 0 to 0.195 eV in graphene occurs at the resonant wavelength of 4.2 μm. This is in the vicinity of, but shifted from, the originally targeted operation wavelength for the Salisbury screen at 3.2 μm. This can be understood by noting that the changes in reflectance that occur upon application of a gate bias can be expressed as a product of two contributions

$$\frac{\Delta R}{\Delta V} = \left(\frac{\Delta R}{\Delta \sigma}\right)\left(\frac{\Delta \sigma}{\Delta V}\right) \tag{4}$$

The first bracketed term on the right side of the equation is purely optical in nature and quantifies the change in reflectance for a given change in graphene's conductivity. The second term is electrical in nature and quantifies the change in conductivity with a change in the applied voltage. The changes in $(\Delta R/\Delta\sigma)$

DOI: 10.1021/nl503431d
Nano Lett. 2015, 15, 1570−1576

can be calculated from the transfer matrix model for any position of the graphene screen and any wavelength of interest. Figure 4b plots the simulated dependence of the reflectance on conductivity that is obtained with the fabricated Salisbury screen and for three neighboring resonance wavelengths of 2.7, 3.2, and 4.2 μm. The plot highlights that the screen could have achieved unity absorption if the graphene had a conductivity in the millisiemens range. The inset shows that for typical conductivity values of graphene (0−100 μS), an almost linear dependence of the reflectance on conductivity is observed. The largest magnitude of $(\Delta R/\Delta\sigma)$ is indeed observed for the wavelength of 3.2 μm. To analyze this further, Figure 4c plots the magnitude of $(\Delta R/\Delta\sigma)$ versus the illumination wavelength. This quantity is largest when the illumination wavelength meets the Salisbury screen condition ($\lambda \approx 4tn_{\mathrm{Spacer}}$) and the magnitude of the electric field is maximized at the location of the screen (Figure 1b). Figure 1b also shows the field profiles for the other resonance wavelengths of 2.7 and 4.2 μm, which show similar standing wave amplitudes of the electric field but lower amplitudes of the field at the location of the graphene sheet. The magnitude of the second term in eq 4 $(\Delta\sigma/\Delta V)$ and its spectral dependence can be understood by analyzing Figure 2b. This figure shows that the largest changes in conductivity upon electrical gating occur for photon energies E_{ph} below E_{F}, that is, on the long wavelength side of the spectrum. The changes in conductivity are particularly large in this spectral range as electrical gating can directly impact the ability of light induced interband transitions. This explains why the largest changes in $(\Delta R/\Delta V)$ occur at a wavelength red-shifted with respect to the Salisbury screen condition for which $(\Delta R/\Delta\sigma)$ is maximized. Indeed, the reflectance changes for the largest bias voltage of 2.6 V used in this study is highest at 4.2 μm instead of 3.2 μm. However, as the gate voltage (and thus E_{F}) is increased, one can achieve large changes in conductivity at increasingly high photon energies (i.e., long wavelengths). This can be seen by analyzing the Figures 3a and 4a. Figure 3a shows that for a value of E_{F} of 0.5 eV the largest reflection change would have been observed at 3.2 μm. Figure 4a further shows that in going from 2 to 2.6 V the conductivity changes with increasing voltage $(\Delta\sigma/\Delta V)$ are also maximized at 3.2 μm. These changes are very significant for a single layer screen and amount to approximately 3.3% per volt.

In conclusion, we have demonstrated that light absorption in a graphene sheet can be enhanced over a suspended sheet by almost a factor of 4 by placing it in a Salisbury screen configuration. Because of the presence of a finite thickness of ionic gel, it is further possible to boost the absorption enhancement within graphene to a factor of 5.5. These enhancements are beneficial for active devices where the absorption is required to be modulated. To verify this point, we first demonstrated that the carrier density in the graphene layer can be actively tuned by electrically gating with an ionic liquid/gel. This causes substantial changes in the position of the Fermi level and thus the conductivity of the graphene. A significantly large modulation of absorption in graphene per applied voltage of 3.3%/V has been demonstrated. This is the highest modulation attained so far in a device that features an atomically thick active layer. It is in part due to the more effective electrical gating with the gel and in part because the presence of the thin ionic gel induces an unexpected and desirable coherent absorption effect that boosts the absorption in the graphene by another 40%. This value and the absolute magnitude of the modulation could be further increased by using higher mobility graphene and by capitalizing on plasmonic resonance supported by patterned graphene.[15,19] The work adds to the increasingly important area of research focused on manipulating electrically tunable coherent optical absorption in two-dimensional solids and metasurfaces.

AUTHOR INFORMATION

Corresponding Author

*E-mail: Brongersma@stanford.edu.

Author Contributions

The manuscript was written through contributions of all authors. All authors have given approval to the final version of the manuscript.

Notes

The authors declare no competing financial interest.

ACKNOWLEDGMENTS

V.T., J.K., K.M.M., and M.L.B acknowledge support from the Department of Energy Grant DE-FG07-ER46426. H.T.Y., H.Y.H., and Y.C. acknowledge the support from the Department of Energy, Office of Basic Energy Sciences, Division of Materials Sciences and Engineering, under contract DE-AC02-76SF00515.

REFERENCES

(1) Novoselov, K. S.; Geim, A. K.; Morozov, S. V.; Jiang, D.; Zhang, Y.; Dubonos, S. V.; Grigorieva, I. V.; Firsov, A. A. *Science* **2004**, *306*, 666−669.

(2) Nair, R. R.; Blake, P.; Grigorenko, A. N.; Novoselov, K. S.; Booth, T. J.; Stauber, T.; Peres, N. M. R.; Geim, A. K. *Science* **2008**, *320*, 1308.

(3) Vakil, A.; Engheta, N. *Science* **2011**, *332*, 1291−1294.

(4) Zhang, Y.; Tang, T. T.; Girit, C.; Hao, Z.; Martin, M. C.; Zettl, A.; Crommie, M. F.; Shen, Y. R.; Wang, F. *Nature* **2009**, *459*, 820−823.

(5) Bolotin, K. I.; Siks, K. J.; Jiang, Z.; Klima, M.; Fudenberg, G.; Hone, J.; Kim, P.; Stormer, H. L. *Solid State Commun.* **2008**, *146*, 351−355.

(6) Lee, C.; Wei, X.; Kysar, J. W.; Hone, J. *Science* **2008**, *321*, 385−388.

(7) Li, X.; Zhu, Y.; Cai, W.; Borysiak, M.; Han, B.; Chen, D.; Piner, R. D.; Colombo, L.; Ruoff, R. S. *Nano Lett.* **2009**, *9*, 4359−4363.

(8) Wang, X.; Zhi, L.; Müllen, K. *Nano Lett.* **2008**, *8*, 323−327.

(9) Xia, F.; Mueller, T.; Lin, Y. M.; Valdes-Garcia, A.; Avouris, P. *Nat. Nanotechnol.* **2009**, *4*, 839−843.

(10) Mueller, T.; Xia, F.; Avouris, P. *Nat. Photonics* **2010**, *4*, 297−301.

(11) Ju, L.; Geng, B.; Horng, J.; Girit, C.; Martin, M.; Hao, Z.; Bechtel, H. A.; Liang, X.; Zettl, A.; Shen, Y. R.; Wang, F. *Nat. Nanotechnol.* **2011**, *6*, 630−634.

(12) Greffet, J. J. *Nature* **2011**, *478*, 191−192.

(13) Echtermeyer, T. J.; Britnell, L.; Jasnos, P. K.; Lombardo, A.; Gorbachev, R. V.; Grigorenko, A. N.; Geim, A. K.; Ferrari, A. C.; Novoselov, K. S. *Nat. Commun.* **2011**, *2*, 1−5.

(14) Fang, Z.; Liu, Z.; Wang, Y.; Ajayan, P. M.; Nordlander, P.; Halas, N. J. *Nano Lett.* **2012**, *12*, 3808−3813.

(15) Thongrattanasiri, S.; Koppens, F. H. L.; García de Abajo, F. J. *Phys. Rev. Lett.* **2012**, *108*, 1−5.

(16) Liu, M.; Yin, X.; Ulin-Avila, E.; Geng, B.; Zentgraf, T.; Ju, L.; Wang, F.; Zhang, X. *Nature* **2011**, *474*, 64−67.

(17) Furchi, M.; Urich, A.; Pospischil, A.; Lilley, G.; Unterrainer, K.; Detz, H.; Klang, P.; Andrews, A. M.; Schrenk, W.; Strasser, G.; Mueller, T. *Nano Lett.* **2012**, *12*, 2773−2777.

(18) Woo, J. M.; Kim, M. S.; Kim, H. W.; Jang, J. H. *Appl. Phys. Lett.* **2014**, *104*, 1−4.

(19) Jang, M. S.; Brar, V. W.; Sherrott, M. C.; Lopez, J. J.; Kim, L.; Kim, S.; Choi, M.; Atwater, H. A. *Phys. Rev. B* **2014**, *90*, 1−5.

DOI: 10.1021/nl503431d
Nano Lett. 2015, 15, 1570−1576

(20) Fante, R. L.; McCormack, M. T. *IEEE Trans. Antennas Propag.* **1988**, *36*, 1443−1454.
(21) Munk, B. A. *Frenquency Selective Surfaces: Theory and Design*; John Wiley & Sons: New York, 2000; pp 315−317.
(22) Majumdar, A.; Kim, J.; Vuckovic, J.; Wang, F. *Nano Lett.* **2013**, *13*, 515−518.
(23) Chen, F.; Qing, Q.; Xia, J.; Li, J.; Tao, N. *J. Am. Chem. Soc.* **2009**, *131*, 9908−9909.
(24) Geim, A. K.; Novoselov, K. S. *Nat. Mater.* **2007**, *6*, 183−191.
(25) Ye, J.; Craciun, M. F.; Koshino, M.; Russo, S.; Inoue, S.; Yuan, H.; Shimotani, H.; Morpurgo, A. F.; Iwasa, Y. *Proc. Natl. Acad. Sci. U.S.A.* **2011**, *108*, 13002−13006.
(26) Luryi, S. *Appl. Phys. Lett.* **1988**, *52*, 501−503.
(27) Xia, J.; Chen, F.; Li, J.; Tao, N. *Nat. Nanotechnol.* **2009**, *4*, 505−509.
(28) Das, A.; Pisana, S.; Chakraborty, B.; Piscanec, S.; Saha, S. K.; Waghmare, U. V.; Novoselov, K. S.; Krishnamurthy, H. R.; Geim, A. K.; Ferrari, A. C.; Sood, A. K. *Nat. Nanotechnol.* **2008**, *3*, 210−215.
(29) Zhang, Y.; Tan, Y.-W.; Stormer, H. L.; Kim, P. *Nature* **2005**, *438*, 201−204.
(30) Hanson, G. W. *J. Appl. Phys.* **2008**, *103*, 1−8.
(31) Falkovsky, L. A.; Pershoguba, S. S. *Phys. Rev. B* **2007**, *76*, 1−4.
(32) Li, Z. Q.; Henriksen, E. A.; Jiang, Z.; Hao, Z.; Martin, M. C.; Kim, P.; Stormer, H. L.; Basov, D. N. *Nat. Phys.* **2008**, *4*, 532−535.
(33) Falkovsky, L. A. *J. Phys. Conf. Ser.* **2008**, *129*, 1−7.
(34) Saleh, B. E. A.; Teich, M. C. *Fundamentals of Photonics*, 2nd ed.; Wiley Interscience: Hoboken, NJ, 2007.
(35) Garcia de Abajo, F. J. *ACS Photonics* **2014**, *1*, 135−152.

DOI: 10.1021/nl503431d
Nano Lett. 2015, 15, 1570−1576